



ELSEVIER



<https://doi.org/10.1016/j.ultrasmedbio.2018.09.014>

● *Original Contribution*

MULTIPLE-EXPOSURE DRUG RELEASE FROM STABLE NANODROPLETS BY HIGH-INTENSITY FOCUSED ULTRASOUND FOR A POTENTIAL DEGENERATIVE DISC DISEASE TREATMENT

KHOI NGUYEN,* HSUAN-YEH PAN,^{†,1} KEVIN HAWORTH,^{*,†} ERIC MAHONEY,^{*,2}

KARLA P. MERCADO-SHEKHAR,[†] CHIA-YING LIN,[‡] ZHE ZHANG,[§] and YOONJEE C. PARK^{*,§}

* Department of Biomedical Engineering, University of Cincinnati, Cincinnati, Ohio, USA; [†] Department of Internal Medicine, University of Cincinnati, Cincinnati, Ohio, USA; [‡] Department of Orthopaedic Surgery, University of Cincinnati, Cincinnati, Ohio, USA; and [§] Department of Chemical & Environmental Engineering, University of Cincinnati, Cincinnati, Ohio, USA

(Received 13 April 2018; revised 10 September 2018; in final form 17 September 2018)

Abstract—The combination of simvastatin and CF680 dye encapsulated by stable nanodroplets has been developed as a drug delivery carrier. Simvastatin has previously been found to be a potential degenerative disc disease treatment. Multiple exposures of the nanodroplets to high-intensity focused ultrasound induced release of simvastatin. Each ultrasound exposure yielded a consistent concentration of the drug and dye released. B-mode ultrasound image analysis data and cavitation data clearly indicated the release mechanism is phase transition of the liquid nanodroplets into gas bubbles. The nanodroplets were stably stored in *ex vivo* rabbit spinal discs for at least 14 days, and the contents responded to ultrasound exposure on demand. Lastly, nucleus pulposus cells harvested from rabbit spine discs and exposed to media with nanodroplets exhibited a decrease in cell viability (85%) relative to the cells only (96.7%) at 24 h, but no difference at 48 h. Thus, the system may be a potential degenerative disc disease treatment. (E-mail: parkye@ucmail.uc.edu) © 2018 World Federation for Ultrasound in Medicine & Biology. All rights reserved.

Key Words: High-intensity focused ultrasound, On-demand drug release, Multiple releases, Degenerative disc disease.

INTRODUCTION

Degenerative disc disease (DDD) refers to symptoms of back or neck pain caused by wear-and-tear on a spinal disc. Approximately 80% of the adult population will experience low back pain associated with DDD throughout their lifetime (Health Quality Ontario 2006; Hicks et al. 2009). Current therapeutic interventions for degenerated intervertebral discs (IVDs) are intradiscal injections of non-steroidal anti-inflammatory medications or epidural steroidal medications, which require repeated injections throughout the lifetime to reduce chronic pain (Mae et al. 2012). These treatments last about 3 months depending on pain level. Open surgery is considered when these less invasive treatments, that is, intradiscal

injections, fail. Unfortunately, 20% of the patients are still in pain after surgery, and 7% to 15% develop failed back syndrome, resulting in foraminal stenosis, painful disc and pseudarthrosis (Schofferman et al. 2003; Volpentesta et al. 2014).

Recent emphasis has been directed at the reversal of disc degeneration or replacement of the affected disc by using biological materials, including growth factors, stem cells and gene transplant (Taher et al. 2012; Than et al. 2014). We previously reported that simvastatin, a 3-hydroxy-3-methylglutaryl coenzyme A reductase inhibitor, enhances chondrogenesis of intervertebral disc cells, which in turn facilitates the repair of degenerative IVDs in a developed animal model (Than et al. 2014). However, the efficacy associated with local simvastatin injection can be transient if adequate vehicles are not used to provide sustainable release. There is a critical need to assess feasible options that can deliver hydrophobic simvastatin and control the release site-specifically, especially when the disease condition changes over time.

Address correspondence to: Yoonjee Park, Department of Chemical & Environmental Engineering, University of Cincinnati, 2901 Woodside Drive, Cincinnati, OH 45221, USA. E-mail: parkye@ucmail.uc.edu

¹ Current address: School of Optometry, Indiana University, Bloomington, IN 47405

² Current address: PO Box 100942, Arlington, VA 22210, USA.

Ultrasound-mediated drug release is a potential solution. High-intensity focused ultrasound (HIFU) generates pressure waves that can phase-transition liquid perfluorocarbon droplets into gas bubbles, a process called acoustic droplet vaporization (ADV) (Fabiilli *et al.* 2009; Kripfgans *et al.* 2000; Sheeran *et al.* 2011). When the droplets undergo ADV, phase-transitioned gas bubbles can release the drug (Fabiilli *et al.* 2010a, 2010b; Moncion *et al.* 2017; O'Neill and Rapoport 2011; Rapoport *et al.* 2009a, 2009b, 2010; Sheeran *et al.* 2011), and the bubbles can be detected by ultrasound imaging because of their echogenicity (Fabiilli *et al.* 2009; Goldberg 1996; Park *et al.* 2012). In this study, we investigated the potential of using a double emulsion technique to stably encapsulate hydrophobic simvastatin in perfluorocarbon liquid droplets at body temperature and release the simvastatin at select times with consistent dosage using multiple temporally spaced HIFU exposures. The cytotoxicity of the nanodroplets in physiologic conditions and triggered release in *ex vivo* rabbit discs were also investigated. The study addresses an important gap in knowledge of developing and quantifying hydrophobic drug delivery *in vitro* using HIFU for multiple uses.

METHODS

Nanodroplet materials and synthesis

The nanodroplets were synthesized *via* a double-emulsion process of drug-containing water droplets in perfluorocarbon, which was emulsified in water. The first emulsion of water droplets containing simvastatin powder at a concentration of 100 mg/mL and a total mass of 2.4 mg was dispersed in liquid perfluoropentane (1.55 mL) (Synquest Laboratories, Alachua, FL, USA) with Krytox (150 μ L) (DuPont, USA) as polymer surfactant *via* probe sonication (Vibra Cell 400, Sonics, Newtown, CT, USA) at an amplitude of 20% for 3 min with 10-s on and 20-s pause in an ice bath. It should be noted that simvastatin powder was used rather than solubilized simvastatin because of the low solubility of hydrophobic simvastatin in water. Care was taken to ensure that the simvastatin powder was uniformly dispersed in the water before emulsification to form water droplets in perfluoropentane. The second emulsion was then created by adding liposomes in de-ionized (DI) water to the first emulsion and probe-sonicating in an ice bath in the same manner. The liposome components consisted of 1,2-dipalmitoyl-*sn*-glycero-3-phosphocholine (DPPC; Avanti Polar Lipids, Inc., Alabaster, AL, USA) and 1,2-distearoyl-*sn*-glycero-3-phosphoethanolamine-*N*-[methoxy(polyethylene glycol)-5000] (DSPE-PEG 5 K; Nanocs, Boston, MA, USA) at a 85:15 mole ratio dissolved in chloroform (10 mg/mL). The chloroform was evaporated in a chemical hood. The dried film

was hydrated with DI water at 5.62 μ mol/mL and probe-sonicated at room temperature for 10 min to form liposomes. The resulting solution was washed three times by centrifugation (2700 rpm) and replacement of the supernatant with DI water. The final product consists of water droplets in perfluoropentane droplets dispersed in water (W1/O/W2). Simvastatin was substituted with a dye (rhodamine B or CF680) or co-encapsulated with a dye in the W1 phase.

Characterization of nanodroplets: Optical imaging and spectroscopy

Differential interference contrast (DIC) and fluorescence microscopy with an oil-immersion objective lens \times 63 (Carl Zeiss, Inc., Oberkochen, Germany) were used to determine drug/dye encapsulation of the nanodroplets optically. Dynamic light scattering (DLS) (NanoBrook Omni, Brookhaven Instruments, Holtsville, NY, USA) was used to determine the hydrodynamic diameter of the nanodroplets. A UV–Vis/fluorescence spectrometer (SpectraMax, Molecular Devices, LLC, San Jose, CA, USA) was used to detect simvastatin and CF680 dye by observing peaks at 237 nm (Alvarez-Lueje *et al.* 2005; Merienne *et al.* 2017) for UV and 680 nm for fluorescence, respectively.

Stability test

Nanodroplets in DI water or cell culture medium (Dulbecco's Modified Eagle Medium: Nutrient Mixture F-12 [DMEM/F-12] supplemented with 10% fetal bovine serum (FBS) and 1% penicillin–streptomycin solution) were stored in an incubator at 37°C for 2 wk. Every 3 d, 10 μ L of droplets from each vial were withdrawn and diluted 1000 times. Diluted droplets (10 μ L) were placed in a hemocytometer and counted using a microscope with an objective lens \times 40 in phase-contrast mode (Axio Observer A1, Carl Zeiss, Inc, Oberkochen, Germany). Because of the diffraction limit in resolution, particle sizes < 400 nm were not considered. Dynamic light scattering (DLS) was used to monitor the stability of the nanodroplets against aggregation, rupture or dissolution by size measurement (Rovers *et al.* 2015). When the nanodroplets undergo phase transition, multiple peaks in the size distribution appear corresponding to droplets, bubbles (from droplets that phase-transition) and shell fragments after dissolution. Bubbles are anticipated to be >1 μ m (Bardin *et al.* 2011), shell fragments <100 nm (Rovers *et al.* 2015) and droplets near 400–500 nm. The particle size that DLS can measure ranges from <0.3 nm to 10 μ m. Nanodroplets (150 μ L) in water solution were diluted in 1.35 mL of DI water for the measurements. Three measurements were taken for each sample and averaged over time for 21 d.

Ultrasound exposure of nanodroplets

The nanodroplets encapsulating dye or drug were placed in a 1.5-mL conical tube. The conical tube was placed in the focal volume of an ultrasound transducer (H104, Sonic Concepts, Bothell, Washington, USA) using pulse-echo alignment and exposed to ultrasound in a tank of degassed water at 37°C. The ultrasound had a center frequency of 500 kHz, peak negative pressure of 3 MPa (free field), pulse duration of 10 cycles and pulse repetition frequency of 100 Hz. Each sample was insonified using the following exposure schemes.

Single exposure. Each sample vial had a volume of 2 mL and was exposed to ultrasound for 2 min. The control sample (sham exposure) was placed inside of the tank but was not exposed to ultrasound. Each sample was centrifuged at 4000g for 3 min to collect released dye/drug in the supernatant.

Multiple exposures. Each sample underwent the same procedure as for a single exposure. However, after centrifugation and removal of 300 μ L of the supernatant, 300 μ L of DI water was added to resuspend the pellet. Ultrasound exposure, centrifugation and reservation of the supernatant were repeated three more times. Control trials (sham exposure) were performed by repeating the above procedure, but setting the ultrasound exposure to 0 MPa.

UV–visual absorbance for drug release analysis

The supernatant from ultrasound exposure was mixed with the same volume of acetonitrile (*i.e.*, 1:1 [v/v] ratio of water and acetonitrile) to dissolve simvastatin possibly in the lipid shell debris and determine the concentration of simvastatin. Acetonitrile was used to disrupt the lipid aggregation structure because it is a commonly used solvent in high-performance liquid chromatography analysis, which uses UV–Vis for concentration quantification (Reis et al. 2013). The mixture was transferred into a well of a UV-transparent 96-well plate, and its optical absorbance was measured at 237 nm using a UV-Vis plate reader (SpectraMax, Molecular Devices, LLC, San Jose, CA, USA). The concentration of simvastatin was calculated from the measured optical absorbance based on a standard calibration (Supplementary Fig. S1, online only).

In vivo imaging system (IVIS) for dye release analysis

A Bruker MultiSpectral FX (Bruker, Carestream) Fluorescence/X-ray Multimodality Imaging system was used to visualize dye CF680 release from the nanodroplets by ultrasound exposure. MATLAB (The MathWorks, Natick, MA, USA) was used to quantitatively analyze the average intensity within each vial.

B-Mode ultrasound imaging and cavitation imaging

B-Mode and passive cavitation data were acquired using an L7-4 linear array (Philips) and Vantage 256 ultrasound research scanner (Verasonics). The L7-4 linear array provides millimeter to sub-millimeter lateral resolution (Haworth et al. 2017). Additionally, because the fundamental insonation frequency (500 kHz) is well outside the bandwidth of the L7-4 linear array, the receive gain can be increased without saturating the analogue-to-digital converters. The increased receive gain improves the signal-to-noise ratio of the measurement. The average echogenicity of a region of interest (ROI) in the B-mode image of each centrifuge tube containing droplets before, during and after ultrasound exposure was computed for each of the four ultrasound exposures performed and for the four sham (no ultrasound) exposures. For each exposure, five samples were insonified (*i.e.*, $n = 5$). In preliminary experiments, harmonics were observed from 1.5 to 8.5 MHz; however, a drop in broadband emissions was observed at approximately 2 and 8 MHz. Therefore, passive cavitation images were produced (Haworth et al. 2017) to quantify the magnitude of cavitation activity integrated over all frequencies between 2 and 8 MHz during each of the ultrasound exposures (and the sham exposures). The total power in an ROI in the passive cavitation image of each centrifuge tube was computed.

Emulsion stability and ultrasound response in ex vivo rabbit discs

A 9- to 10-wk-old female New Zealand White rabbit was killed, and the spine was extracted. All surgical procedures followed an approved animal IACUC protocol from the University of Cincinnati, Laboratory Animal Medical Services. Dye CF680R-encapsulated nanodroplets were injected into the intervertebral discs. After 14 d of incubation, ultrasound with the same setup described earlier was applied to the nanodroplets within the disc space. IVIS was performed to confirm injection of the nanodroplets within the disc space and the feasibility for storage of the nanodroplets within the space overtime.

Cytotoxicity in in vitro rabbit nucleus pulposus cells

The lumbar vertebral column from a female Sprague Dawley rat (250–300 g) was removed and placed in ice-cold phosphate-buffered saline (PBS: 10 mM PO_4^{3-} , 137 mM NaCl and 2.7 mM KCl). All surgical procedures followed an approved animal IACUC protocol at the University of Cincinnati, Laboratory Animal Medical Services. The vertebral column was transferred to a 100-mm petri dish with PBS on ice. Vertebral bodies L1/2, L2/3, L3/4 and L4/5 were dissected, and the intervertebral discs removed from the surrounding

dense tissue, cartilaginous endplates and outer annulus fibrosis from each vertebral body. Under sterile conditions, the discs were transferred to a 100-mm petri dish on ice containing 25 mL of equal parts of Dulbecco's Modified Eagle Medium and Ham's F-12 medium (DMEM/F12) containing 5% heat-inactivated FBS with 0.2% pronase and 0.004% deoxyribonuclease II type IV. With a scalpel, discs were minced into pieces of approximately 2 mm³ in volume. The samples contained within the solution were poured into a 50-mL centrifuge tube and placed into a 37°C CO₂ incubator for 1 h under gentle agitation. A small pellet was formed at the bottom of the tube, and the solution was carefully aspirated so as not to disturb the tissue pellet. The pellet was resuspended in 25 mL of DMEM/F12 containing 5% heat-inactivated FBS with bacterial 0.02% collagenase type II and 0.004% deoxyribonuclease II type IV. The sample tube was placed into a 37°C CO₂ incubator overnight. After incubation, the pellet formed at the bottom of the tube was gently mixed then poured over a sterile 70- μ m nylon mesh filter into a new sterile 50-mL Falcon tube. Then, 20 mL of DMEM/F12 medium, 10% FBS and 1% antibiotics were added to the 50-mL tube. The medium containing filtered NP cells was gently mixed, seeded into a 75-cm² flask at a density of 2.5×10^4 cells/cm² and then placed into a 37°C CO₂ incubator for 24 h.

The ReadyProbes Cell Viability Imaging Kit, Blue/Green was used to assay cytotoxicity (cell viability) of the nanodroplets. Hoechst 33342 (blue filter) and Nuc-Green Dead reagent (green filter) were used for live and dead cell staining, respectively. The *red* color in the image in Section Cytotoxicity was used instead of *green* for dead cells for color contrast using ImageJ software (National Institute of Health, Bethesda, MD, USA). Cell viability was determined by counting the number of live or dead cells using Image J. Cell viability (%) was determined as 100 times the number of live cells divided by the total number of cells (live cells plus dead cells). The assay was performed in triplicate.

Statistical analysis

Two-way analysis of variance with either Tukey's honest significant difference or Sidak's multiple comparison test was used to statistically analyze data for drug/dye release, B-mode echogenicity and cavitation activity. Student's *t*-test was used for the cytotoxicity data. Error bars represent one standard deviation.

RESULTS

Characterization and stability of nanodroplets

The average size of the nanodroplets measured by DLS was \sim 500 nm in diameter (Figure 1C at day 0). The

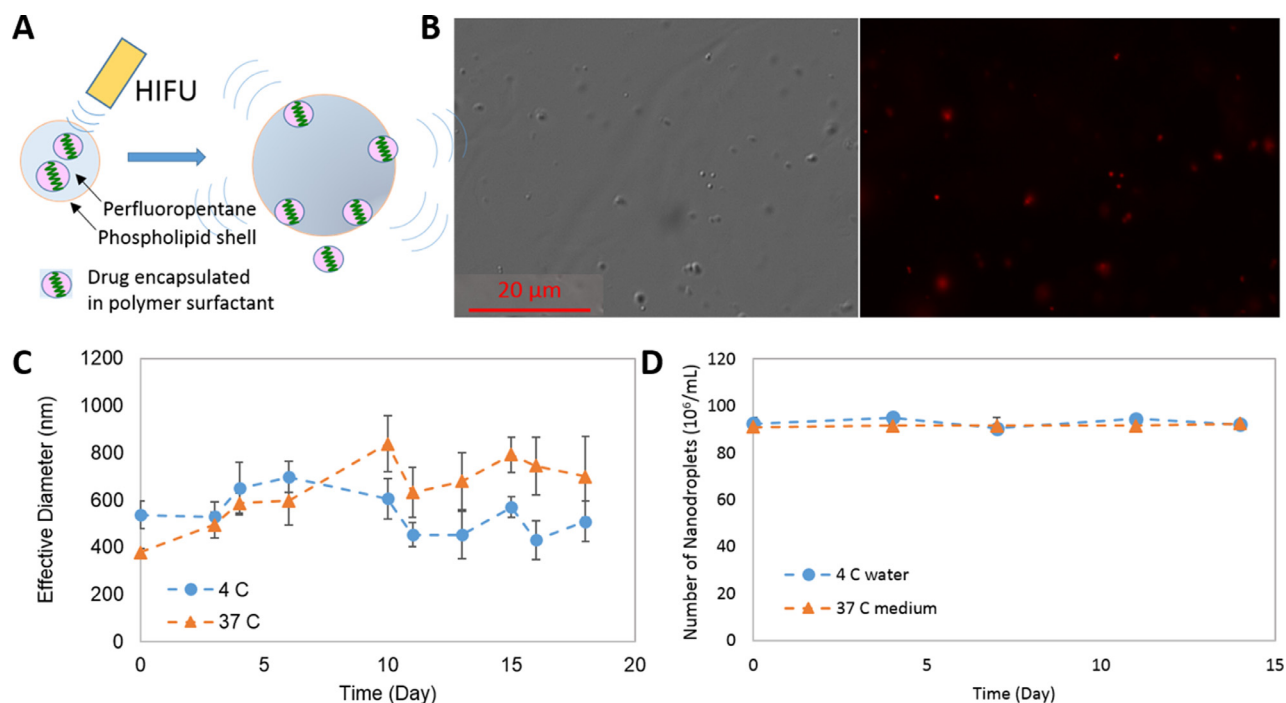


Fig. 1. Cytotoxicity of the nanodroplets compared with that of control (cells only) measured following cell harvest after 24 and 48 h of incubation. The top images are representative images of the live (*blue*)/dead (*red*) assay. The bottom plots provide the average cell viability across all trials ($n = 3$).

nanodroplets observed in the differential interference contrast (DIC) optical image are 300–500 nm in diameter.

When rhodamine B dye was co-encapsulated with simvastatin, the encapsulation inside the nanodroplets was visualized by fluorescence images (Figure 1B, red color in the nanodroplets). UV-Vis data also proved the presence of simvastatin and rhodamine B associated with the nanodroplets as the peaks at wavelengths of 237 and 555 nm, respectively (Merienne et al. 2017; Stobiecka and Hepel 2011).

Only a single peak around 400 nm was observed in the size distribution measured by DLS after storing the droplets in 4°C DI water for 28 d. The lack of larger and smaller peaks indicates that no aggregation, dissolution or fragmentation occurred (Figure 2). A single peak was observed at 18 d when the droplets were stored in 37°C DI water (data not shown). In addition, the number of nanodroplets > 400 nm did not change for at least 14 d at 4°C in water and 37°C in the medium, determined optically (Figure 1D). The size distribution of the nanodroplets stored at 37°C on day 28 revealed peaks at >1000 nm and at ≤100 nm (Figure 2), suggesting that the nanodroplets undergo a phase transition appearing as debris and bubbles.

Multiple-exposure drug/dye release by ultrasound

When the nanodroplets were exposed to HIFU, the optical turbidity of the solution increased (Figure 3A), suggesting acoustic droplet vaporization occurred (Kripfgans et al. 2000; Zhang and Porter 2010). Bubbles were

also observed at the top of the fluid after insonation. Each of the multiple ultrasound exposures resulted in an increase in the measured simvastatin (Figure 3B) or CF680 dye (Figure 3C) relative to sham (no ultrasound) exposures. Figure 3B illustrates that approximately 11 μg/mL simvastatin was released after each exposure. The sham exposure had a release of approximately 5 μg/mL. The difference in the concentration of simvastatin released between the sham and US exposure groups was significant (analysis of variance, p value = 0.0026). The difference in the concentration between the two groups for each individual US insonation was also determined to be significant (p values = 0.0019, 0.0054 and 0.0073 for first, second and third exposures, respectively). Each exposure released approximately 1% of the total amount of encapsulated simvastatin (1.24 mg/mL).

The IVIS measurements indicate that more CF680 dye was released on US exposure relative to sham exposure (Figure 3C, D). Similar to the simvastatin results, consistent amounts of dye were released after each US exposure. The p values between the US and sham groups for each individual exposure were 0.1944, 0.1846, 0.1261 and 0.2252 for first, second, third and fourth exposures, respectively. Large standard deviations may explain why the p values were not significant even though nearly twice as much simvastatin was released with ultrasound relative to no ultrasound exposure. The color intensity decreases with increasing sham exposures, likely because of the dilution that occurs when the supernatant is replaced with DI water.

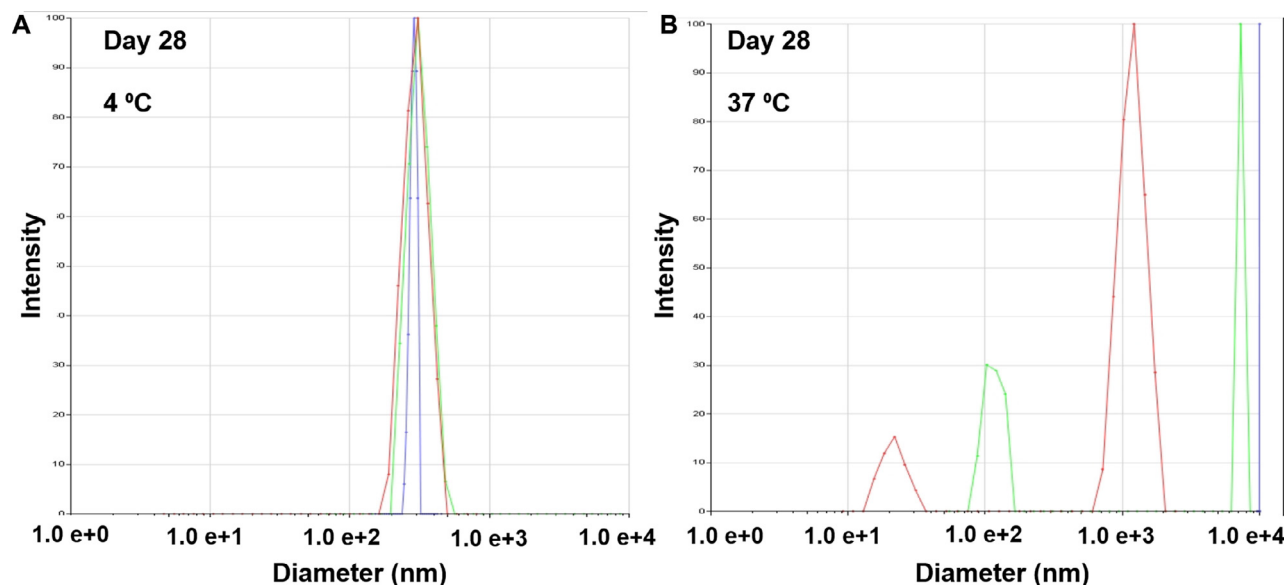


Fig. 2. (A) Schematic of drug release from the nanodroplet *via* phase transition induced by HIFU trigger. (B) Differential interference contrast and fluorescence optical images (63× magnification). (C) Effective (hydrodynamic) diameter measured by dynamic light scattering over time at two different temperatures. (D) Number of nanodroplets counted over time at 4°C and at 37°C in the medium using phase contrast. HIFU = high-intensity focused ultrasound.

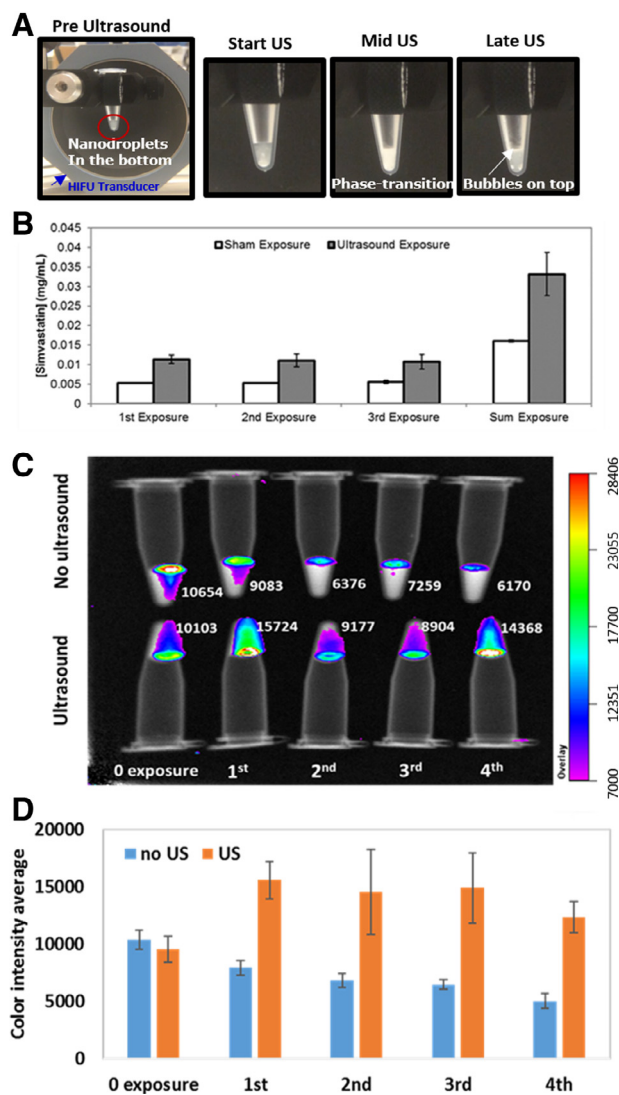


Fig. 3. Dynamic light scattering data: size distributions of the nanodroplets stored at 4°C and 37°C for 28 d. Different-colored curves indicate each measurement ($n = 3$).

B-Mode echogenicity and cavitation activity

After ultrasound exposure, the echogenicity was significantly higher than before US exposure ($p \leq 0.0002$), based on ultrasound B-mode analysis (Figure 4A, B), indicating that microbubbles were produced by phase-transitioning the liquid perfluorocarbon core of the nanodroplets. The echogenicity was also significantly greater after ultrasound exposure compared with after sham treatment ($p < 0.0001$). Even after four exposures, the post-US echogenicity was consistently increased, indicating that not all of the droplets had been converted into bubbles. No change in echogenicity was observed in DI water without nanodroplets.

The passive cavitation spectra acquired during US exposure with the nanodroplets revealed no harmonics,

potentially indicative of strong inertial cavitation (data not shown). Passive cavitation images acquired during US exposure had five orders of magnitude more cavitation in the centrifuge tube compared with images acquired during the sham exposure (Figure 4C), which was statistically significant ($p < 0.0001$ for all comparisons). The sham exposure values were similar to those of the pre- and post-ultrasound exposures and the ultrasound exposure of the centrifuge tube without droplets ($p > 0.9999$ for all time points within each exposure). The measured cavitation activities pre- and post-exposure are indicative of the noise floor of the system. These data indicate that microbubbles were formed and cavitated during insonation of the nanodroplets. In Figure 4C, a relatively high cavitation activity was observed for the pre-US measurement for the first exposure. Manual observation of the ultrasound B-mode image reveals a few sparse bubbles that may have been nuclei for the increased cavitation activity.

Emulsion stability and the ultrasound response in *ex vivo* rabbit discs

Dye-encapsulated nanodroplets injected in *ex vivo* rabbit discs were incubated at 37°C and monitored using IVIS 7 and 14 d after incubation began (Figure 5A). The results indicated that the dye was stored in the discs for at least 14 d. The nanodroplets injected in the whole *ex vivo* spine with ultrasound exposure and no exposure imaged using IVIS after 14 d of incubation also indicated the storage stability in the *ex vivo* disc at least for 14 d (Figure 5B). The dye remained active after ultrasound exposure.

Cytotoxicity

Cytotoxicity of the nanodroplets was assessed on nucleus pulposus cells harvested from the rabbit intervertebral discs. At 24 h, cell viability with and without nanodroplets was $85\% \pm 4.3\%$ and $96.7 \pm 1.1\%$, respectively ($n = 3$). The difference was statistically significant (p value = 0.011). After 48 h of incubation, cell viability did not significantly differ between cells incubated with and without nanodroplets ($56.3 \pm 12.9\%$ and $57.5 \pm 7.9\%$, respectively; p value = 0.463) (Figure 6).

DISCUSSION

Overall, the results from this study indicate that a stable nanodroplet emulsion can release drugs as a result of multiple ultrasound exposures. According to the Antoine equation, with elevated pressure inside the nanodroplet caused by Laplace pressure (Sheeran *et al.* 2011), the boiling point of the perfluoropentane nanodroplet is 32.7°C. The temperature does not fully explain why the nanodroplets did not go through a phase

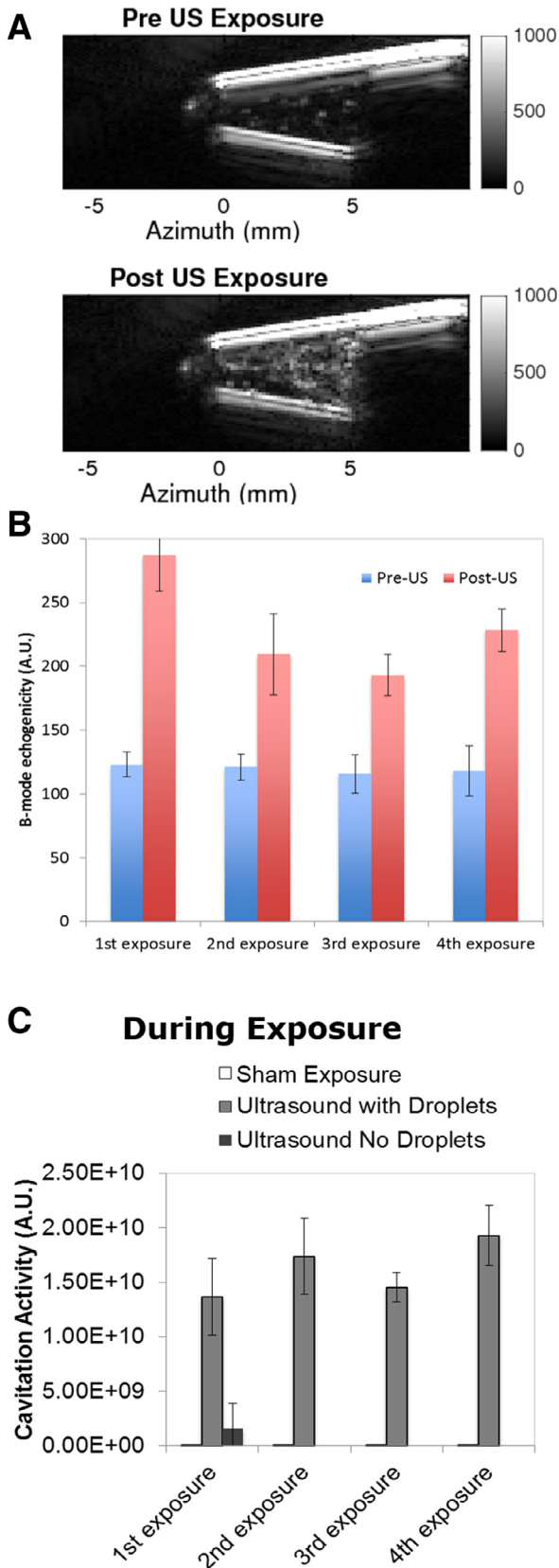


Fig. 4. Release of drug and dye after multiple US exposures (A) Photographs of nanodroplets triggered by HIFU. (B)

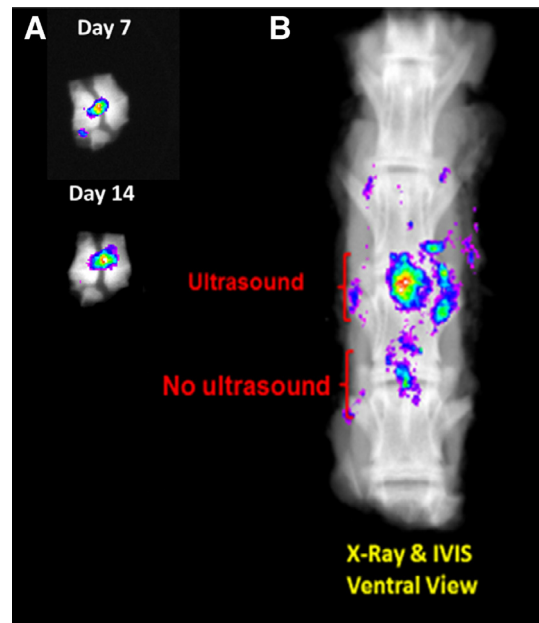


Fig. 5. (A) Ultrasound B-mode images pre- and post-US exposure; (B) Average B-mode echogenicity within the tube before (blue) and after (red) US exposure. (C) Cavitation activity of the nanodroplets before, during and after US and sham exposures. Measurements were made with and without droplets. HIFU = high-intensity focused ultrasound; US = ultrasound.

transition during the first 14 d of incubation at 37°C. Thus, we believe the stability of nanodroplets (*i.e.*, reduced spontaneous vaporization) is in part due to metastability of the superheated perfluorocarbon against bubble nucleation (Delale et al. 2003; Mountford et al. 2015). Over time, if droplets aggregate and merge, it is possible that the boiling point of the larger particles decreases to 37°C or less, and the nanodroplets are no longer stable. Furthermore, we have noticed that mechanical forces such as pipetting, stirring and centrifugation also affected the stability. These phenomena are consistent with observations from other studies (Rapoport et al. 2009a, 2009b), indicating that shear stresses resulting from pipetting can cause a phase transition. For clinical applications for DDD, the nanodroplets will not be affected by mechanical forces except during injection because they will be isolated in the discs.

Both B-mode and passive cavitation imaging provided feedback on the liquid nanodroplet phase transition into gas microbubbles. Ultrasound imaging has been adopted to monitor needle-based injections of ther-

Simvastatin concentrations in the supernatant measured after HIFU exposure. Sham exposure: n = 2, ultrasound exposure: n = 4. (C) Representative IVIS images and color intensity analysis for dye release. The numbers next to each sample represent relative dye concentrations. (D) Average color intensity within each tube (n = 3). HIFU = high-intensity focused ultrasound (IVIS = In Vivo Imaging System).

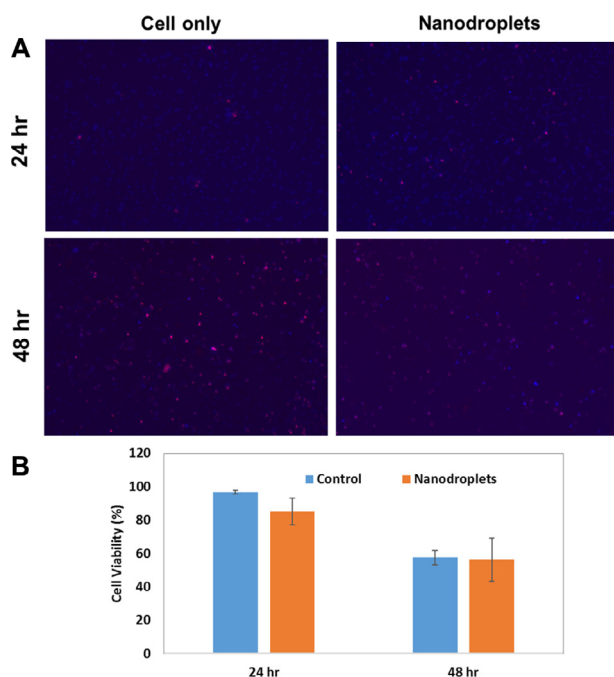


Fig. 6. (A) IVIS images of dye-encapsulated nanodroplets in *ex vivo* rabbit disc at days 7 and 14 of incubation. (B) *Ex vivo* test of high-intensity focused ultrasound trigger of dye-encapsulated nanodroplets after 14 d of incubation after injection into the disc (IVIS = In Vivo Imaging System).

apeutics and also to confirm the phase transition of nanodroplets to bubbles (Kopeček *et al.* 2013; Rapoport *et al.* 2009a, 2009b, 2011). If a strong correlation between drug release and the number of phase-transitioned droplets exists, then the B-mode imaging could be used as a non-invasive metric for drug release.

Each ultrasound exposure resulted in consistent release of both a drug and a dye. Approximately twice as much drug release occurred for ultrasound exposures relative to sham exposures (Figure 3b). A similar ratio was observed for dye release (Figure 3D). The dye released before the first ultrasound exposure (Figure 3D) could be due partly to passive leakage from the droplets or imperfect separations between the supernatant and the nanodroplets. A previous study reported that degenerative discs treated with 5 mg/mL simvastatin in hydrogel exhibited higher gene expression of aggrecan and collagen type II than control (Than *et al.* 2014). A dosage of simvastatin <5 mg/mL has not been tested for chondrogenesis yet. In this study, 0.012 mg/mL simvastatin per each insonation was released, which is 1/100th of the sample. Although the concentration is <5 mg/mL, we found that a consistent amount of simvastatin was released by each ultrasound exposure, meaning multiple exposures will lead to higher dosages effective for chondrogenesis. Please also note that in the cited report, 5 mg/mL simvastatin was loaded in a biodegradable

hydrogel and released in a controlled manner over a 12-wk time span. The transient, effective dose to obtain chondrogenesis would be <5 mg/mL. Further *in vivo* investigation is warranted to evaluate the ultrasound exposure required for the proposed delivery for an efficacious outcome. Furthermore, modification of the droplet properties and ultrasound insonation parameters may lead to greater droplet vaporization efficiency, resulting in more drug release (Fabiilli *et al.* 2010a, 2010b).

It should be noted that the nature of the released dye differs from that of simvastatin, likely because of the relative hydrophobicity of simvastatin compared with the dye. Solubilities of simvastatin and CF680 dye in water are ~0.03 mg/mL (Sigma-Aldrich) and >100 mg/mL (Biotum), respectively. When released, the simvastatin likely precipitated. The occurrence of precipitation is supported by the fact that the post-US simvastatin concentration matched the sham concentration when the ultrasound-exposed sample was centrifuged at 10,000g for 5 min. However, the dye concentration was significantly higher after ultrasound exposure and centrifugation at 10,000g for 5 min than under the sham conditions. The molecular weights of the dye and simvastatin are 3000 and 419 Da, respectively.

A limitation associated with this study is that the difference in molecular weight and hydrophobicity between the drug and dye may require different centrifugation parameters to isolate the released drug or dye in the supernatant versus drug and dye in the droplets. Additionally, it is possible that the hydrophobic drug molecules may have been associated with lipid monolayers after ultrasound exposure, which would affect the ability to separate the released drug from the encapsulated drug using centrifugation and may affect the drug's bioavailability. To better understand this study limitation, we measured the size of particles in the supernatant using dynamic light scattering after 2 min of centrifugation at 2000g, 4000g, 6000g, 8000g and 10,000g. A peak around 70 to 80 nm was observed after 2000g and 4000g centrifugation. The peak disappeared when using 6000g. At 2000g and 4000g, more of the drug was measured using UV absorbance in the supernatant after US exposure relative to sham exposure. The results imply some drug molecules are still encapsulated in debris after phase transition, and depending on the size of the debris, different centrifugation speeds and times may be needed to isolate these drug-loaded debris. This study used 4000g as a balance between ensuring that nanodroplets accrued in the pellet and any drug-loaded debris remained in the supernatant.

The *ex vivo* disc study suggests the feasibility of injecting the nanodroplets into the discs. The dye remained in the disk for 14 d at 37°C. It also implies that the fluorescent nanodroplets can be monitored

after ultrasound exposure using IVIS techniques for future *in vivo* animal experiments.

The *in vitro* data with the harvested nucleus pulposus cells indicated that the nanodroplets are not highly cytotoxic. Minimal cytotoxicity was observed after 24 h of incubation with the nanodroplets. The live cell population naturally decreases because *in vitro* conditions are not favorable for nucleus pulposus cells. Another limitation of this study is the uncertainty of the bioavailability of free simvastatin versus simvastatin that may be associated with lipid particles after droplet vaporization. It has previously been observed that drugs encapsulated in lipid micelles can be delivered to cells (Park et al. 2008). However, because nucleus pulposus cells in culture may not behave identically to *in vivo* nucleus pulposus cells, the bioavailability should be determined *in vivo* experimentally in future studies.

CONCLUSIONS

Overall, we have developed a stable nanodroplet emulsion that can be activated multiple times by ultrasound (HIFU). The activation can be monitored by ultrasound imaging by analyzing B-mode ultrasound and passive cavitation images. The nanodroplets could be used potentially as a long-term drug carrier for disc diseases and had great stability under *ex vivo* conditions, low cytotoxicity and controlled triggered release. This new drug delivery system will be applied to a degenerative disc disease model in the future.

Acknowledgments—This study was partially supported by National Institutes of Health/National Institute of Arthritis and Musculoskeletal and Skin Diseases Grant R01 AR056649. This study was also partially supported by Ohio Lions Eye Research Foundation and NIH KL2 award.

SUPPLEMENTARY DATA

Supplementary data related to this article can be found at <https://doi.org/10.1016/j.ultrasmedbio.2018.09.014>.

REFERENCES

- Alvarez-Lueje A, Valenzuela C, Squella JA, Nunez-Vergara LJ. Stability study of simvastatin under hydrolytic conditions assessed by liquid chromatography. *J AOAC Int* 2005;88:1631–1636.
- Bardin D, Martz TD, Sheeran PS, Shih R, Dayton PA, Lee AP. High-speed, clinical-scale microfluidic generation of stable phase-change droplets for gas embolotherapy. *Lab Chip* 2011;11:3990–3998.
- Delale CF, Hruby J, Marsik F. Homogeneous bubble nucleation in liquids: The classical theory revisited. *J Chem Phys* 2003;118:792–806.
- Fabiilli ML, Haworth KJ, Fakhri NH, Kripfgans OD, Carson PL, Fowlkes JB. The role of inertial cavitation in acoustic droplet vaporization. *IEEE Trans Ultrason Ferroelectr Freq Control* 2009;56:1006–1017.
- Fabiilli ML, Haworth KJ, Sebastian IE, Kripfgans OD, Carson PL, Fowlkes JB. Delivery of chlorambucil using an acoustically-triggered perfluoropentane emulsion. *Ultrasound Med Biol* 2010a;36:1364–1375.
- Fabiilli ML, Lee JA, Kripfgans OD, Carson PL, Fowlkes JB. Delivery of water-soluble drugs using acoustically triggered perfluorocarbon double emulsions. *Pharm Res* 2010b;27:2753–2765.
- Goldberg BB. *Ultrasound contrast agents*. : Taylor & Francis; 1996.
- Haworth KJ, Bader KB, Rich KT, Holland CK, Mast TD. Quantitative frequency-domain passive cavitation imaging. *IEEE Trans Ultrason Ferroelectr Freq Control* 2017;64:177–191.
- Health Quality Ontario. Artificial discs for lumbar and cervical degenerative disc disease—Update: An evidence-based analysis. *Ont Health Technol Assess Ser* 2006;6:1–98.
- Hicks GE, Morone N, Weiner DK. Degenerative lumbar disc and facet disease in older adults: Prevalence and clinical correlates. *Spine* 2009;34:1301–1306.
- Kopechek JA, Park E, Mei CS, McDannold NJ, Porter TM. Accumulation of phase-shift nanoemulsions to enhance MR-guided ultrasound-mediated tumor ablation *in vivo*. *J Healthcare Eng* 2013;4:109–126.
- Kripfgans OD, Fowlkes JB, Miller DL, Eldevik OP, Carson PL. Acoustic droplet vaporization for therapeutic and diagnostic applications. *Ultrasound Med Biol* 2000;26:1177–1189.
- Mae T, Terada T, Haruyama N, Kodaka K, Yamasaki T, Ozaki M, Arashi T, Abe A, Fukuuchi A. Intradiscal pressurized physiologic saline injection drastically reduced pain from cervical and lumbar disc herniation. *J Pain* 2012;13:S89.
- Merienne C, Semely D, Wolff E, Roussiere A, Tafani M, Ramjaun Z, Caturla L. PP-046 A stability indicating hplc-uv method for quantification of simvastatin and detection of its impurities in oral capsules. *Eur J Hosp Pharmacy* 2017;24(Suppl. 1) A221–A22.
- Moncion A, Lin M, O'Neill EG, Franceschi RT, Kripfgans OD, Putnam AJ, Fabiilli ML. Controlled release of basic fibroblast growth factor for angiogenesis using acoustically-responsive scaffolds. *Biomaterials* 2017;140:26–36.
- Mountford PA, Thomas AN, Borden MA. Thermal activation of superheated lipid-coated perfluorocarbon drops. *Langmuir* 2015;31:4627–4634.
- O'Neill BE, Rapoport N. Phase-shift, stimuli-responsive drug carriers for targeted delivery. *Ther Deliv* 2011;2:1165–1187.
- Park JH, Lee S, Kim JH, Park K, Kim K, Kwon IC. Polymeric nanomedicine for cancer therapy. *Prog Polym Sci* 2008;33:113–137.
- Park Y, Luce AC, Whitaker RD, Amin B, Cabodi M, Nap RJ, Szleifer I, Cleveland RO, Nagy JO, Wong JY. Tunable diacetylene polymerized shell microbubbles as ultrasound contrast agents. *Langmuir* 2012;28:3766–3772.
- Rapoport NY, Efros AL, Christensen DA, Kennedy AM, Nam KH. Microbubble generation in phase-shift nanoemulsions used as anticancer drug carriers. *Bubble Sci Eng Technol* 2009a;1:31–39.
- Rapoport NY, Kennedy AM, Shea JE, Scaife CL, Nam KH. Controlled and targeted tumor chemotherapy by ultrasound-activated nanoemulsions/microbubbles. *J Control Release* 2009b;138:268–276.
- Rapoport N, Christensen DA, Kennedy AM, Nam K. Cavitation properties of block copolymer stabilized phase-shift nanoemulsions used as drug carriers. *Ultrasound Med Biol* 2010;36:419–429.
- Rapoport N, Nam KH, Gupta R, Gao Z, Mohan P, Payne A, Todd N, Liu X, Kim T, Shea J, Scaife C, Parker DL, Jeong EK, Kennedy AM. Ultrasound-mediated tumor imaging and nanotherapy using drug loaded, block copolymer stabilized perfluorocarbon nanoemulsions. *J Control Release* 2011;153:4–15.
- Reis A, Rudnitskaya A, Blackburn GJ, Fauzi NM, Pitt AR, Spickett CM. A comparison of five lipid extraction solvent systems for lipiodomic studies of human LDL. *J Lipid Res* 2013;54:1812–1824.
- Rovers TAM, Sala G, van der Linden E, Meinders MJB. Disintegration of protein microbubbles in presence of acid and surfactants: A multi-step process. *Soft Matter* 2015;11:6403–6411.
- Schofferman J, Reynolds J, Herzog R, Covington E, Dreyfuss P, O'Neill C. Failed back surgery: etiology and diagnostic evaluation. *Spine J* 2003;3:400–403.
- Sheeran PS, Luois S, Dayton PA, Matsunaga TO. Formulation and acoustic studies of a new phase-shift agent for diagnostic and therapeutic ultrasound. *Langmuir* 2011;27:10412–10420.
- Stobiecka M, Hepel M. Multimodal coupling of optical transitions and plasmonic oscillations in rhodamine B modified gold nanoparticles. *Phys Chem Chem Phys* 2011;13:1131–1139.

- Taher F, Essig D, Lebl DR, Hughes AP, Sama AA, Cammisa FP, Girardi FP. Lumbar degenerative disc disease: Current and future concepts of diagnosis and management. *Adv Orthop* 2012;2012:7.
- Than KD, Rahman SU, Wang L, Khan A, Kyere KA, Than TT, Miyata Y, Park YS, La Marca F, Kim HM, Zhang H, Park P, Lin CY. Intradiscal injection of simvastatin results in radiologic, histologic, and genetic evidence of disc regeneration in a rat model of degenerative disc disease. *Spine J* 2014;14:1017–1028.
- Volpentesta G, De Rose M, Bosco D, Stroschio C, Guzzi G, Bombardier IC, Chirchiglia D, Plastino M, Romano M, Cristofalo S, Pardatscher K, Lavano A. Lumbar percutaneous intradiscal injection of radiopaque gelified ethanol (Discogel) in patients with low back and radicular pain. *J Pain Relief* 2014;3:145.
- Zhang P, Porter T. An *in vitro* study of a phase-shift nanoemulsion: A potential nucleation agent for bubble-enhanced HIFU tumor ablation. *Ultrasound Med Biol* 2010;36:1856–1866.